UC Irvine
UC Irvine Previously Published Works

Title

Assessing jet-induced spatial mixing in a rich, reacting crossflow

Permalink

https://escholarship.org/uc/item/5s36r291

Journal

Journal of Propulsion and Power, 19(1)

ISSN

0748-4658

Authors

Demayo, TN
Leong, MY
Samuelsen, GS
et al.

Publication Date

2003

DOI

10.2514/2.6098

License

CC BY 4.0

Peer reviewed

Assessing Jet-Induced Spatial Mixing in a Rich, Reacting Crossflow

T. N. Demayo,[*] M. Y. Leong,[†] and G. S. Samuelsen[‡]
University of California, Irvine, Irvine, California 92697-3550
and
J. D. Holdeman[§]
NASA John H. Glenn Research Center at Lewis Field, Cleveland, Ohio 44135

In many advanced low NO_x gas turbine combustion techniques, such as rich-burn/quick-mix/lean-burn (RQL), jet mixing in a reacting, hot, fuel-rich crossflow plays an important role in minimizing all pollutant emissions and maximizing combustion efficiency. Assessing the degree of mixing and predicting jet penetration is critical to the optimization of the jet injection design strategy. Different passive scalar quantities, including carbon, oxygen, and helium, are compared to quantify mixing in an atmospheric RQL combustion rig under reacting conditions. The results show that the O_2-based jet mixture fraction underpredicts the C-based mixture fraction due to jet dilution and combustion, whereas the He tracer overpredicts it possibly due to differences in density and diffusivity. The He method also exhibits significant scatter in the mixture fraction data that can most likely be attributed to differences in gas density and turbulent diffusivity. The jet mixture fraction data were used to evaluate planar spatial unmixedness, which showed good agreement for all three scalars. This investigation suggests that, with further technique refinement, either O_2 or a He tracer could be used instead of C to determine the extent of reaction and mixing in an RQL combustor.

Nomenclature

d = orifice axial length
f = jet mixture fraction
f_{av} = area-weighted average jet mixture fraction specific to each plane
f_{var} = variance of all point f values in a plane with respect to f_{av}
f_{Xi} = jet mixture fraction based on molar fraction (or concentration) of species i
f_{Yi} = jet mixture fraction based on mass fraction of species i
J = jet to crossflow momentum-flux ratio
M_i = molar mass of species i
R = radius of the quick-mix module
U_S = spatial unmixedness
X_i = molar fraction of species i
x = axial distance from the leading edge of the orifices
Y_i = mass fraction of species i
ϕ = equivalence ratio, $(fuel/air)_{local}/(fuel/air)_{stoichiometric}$

Introduction

MANY advanced low NO_x combustion techniques, such as lean premixed prevaporized injection, lean direct injection, and rich-burn/quick-mix/lean-burn (RQL) rely on the rapid and thorough mixing of air and fuel to minimize all pollutant emissions and maximize combustion efficiency. Various studies have found that fuel–air ratio nonuniformities significantly affect NO_x emissions.[1−3]

In gas turbine combustion, jet mixing in a reacting, hot, fuel-rich crossflow plays an important role due to air jet injection in the primary, secondary, and dilution zones of the combustor. Assessing the degree of mixing and predicting jet penetration are especially critical in the RQL combustion concept. One of the advantages of RQL over other combustion techniques is quick and complete mixing between the rich and lean zones of the combustor to eliminate hot, near-stoichiometric reactant pockets that may lead to NO_x formation. In addition to combustion, the assessment of jet mixing into a crossflow can be applied to a wide range of fields such as gas turbine cooling and staging, fuel–air premixing, vertical short takeoff and landing aircraft, and pollutant discharge from stacks or pipes.

This study compares the use of different scalar quantities, including carbon, oxygen, and an inert tracer gas to quantify mixing in an atmospheric RQL combustion rig under reacting conditions.

Background

Most experimental jet-in-crossflow studies have focused on nonreacting systems, with only a limited number of tests having been reported under reacting conditions. Although isothermal testing is useful and convenient, actual combustor mixing and performance need to be measured in a combusting flow. An extensive listing of these isothermal and reacting studies can be found in Refs. 4–7.

The diagnostic technique chosen to determine mixing in reacting systems is important to the outcome of this study. Qualitative characterization of the mixing process can be inferred through the measurement of temperature profiles and species concentrations. However, to determine the true extent of mixing in a reactant flowfield, one needs to experimentally measure the jet mixture fraction f.

Two techniques, used in numerous studies and summarized by Jones et al.,[8] can be used to measure or deduce f in a transverse flow. The first method is to use nonintrusive optical diagnostics, such as laser-induced fluorescence, Rayleigh scattering (see Refs. 9 and 10), or Raman scattering to quantify spatial and temporal unmixedness. Planar imaging eliminates the need for extractively measuring multiple species and for sampling at multiple points in the flame. However, optical methods are limited by the availability of costly laser and detector systems, the practicality of optical access into the

[*]Research Assistant, Combustion Laboratory.
[†]Research Assistant, Combustion Laboratory; currently Research Engineer, Energy Systems Group, United Technologies Research Center, East Hartford, CT 06108.
[‡]Professor, Combustion Laboratory. Associate Fellow AIAA.
[§]Senior Research Engineer, Combustion Branch, Turbomachinery and Propulsion Systems Division. Associate Fellow AIAA.

flow, the need to seed or modify the fuel to obtain the desired optical signal, and in-flame interferences such as molecular quenching.

The second approach, which is the focus of this study, is based on the measurement of a conserved scalars are quantities unaffected by the chemical reaction, such as carbon, oxygen, nitrogen, or hydrogen mass fraction, equivalence ratio, or an inert gas. This treatment assumes that the slowest chemical kinetic reaction rate is much faster than the turbulent mixing timescales.[11] Under this assumption, local instantaneous composition measurements correspond to chemical equilibrium and can be related to a strictly conserved scalar variable. Furthermore, this technique assumes a well-mixed recirculation zone in which mixing times are much less than residence times.[11]

Previous studies[8,12,13] have used carbon mass fraction and equivalence ratio to calculate f. Aspirated emissions samples were analyzed for CO, CO_2, O_2, total hydrocarbons (THCs), and, in the case of Jones et al.,[8] H_2. These analyses directly capture all carbon-carrying species needed to determine a C-based f. However, in the case of a jet in a rich crossflow, other quantities, such as the oxygen atom O, the oxygen molecule O_2, or an inert tracer gas such as helium He or neon Ne, can be used to simplify the calculation of f. With respect to O_2, because it is a key participant in the combustion reactions, it cannot truly be considered a conserved scalar. However, because it is only present in the jet flow and because there is considerable excess air present in the downstream flow, its concentration profile can not only be used to indicate jet presence and dispersion, as was shown in Refs. 12 and 13, but potentially the mixture fraction as well.

Helium has served as an inert tracer in various studies to determine a wide range of parameters, such as groundwater transport,[14] fluid flow in a porous rock,[15] residence time in a spray-drying tower,[16] automobile exhaust flow rate,[17] impervious wall effectiveness of film-cooling slots,[18] scalar flowfield in a combustor rig under isothermal (nonreacting) conditions,[11,19,20] and mass transport rates in a nonreacting jet-in-crossflow.[21,22] Helium is an inexpensive, readily available gas that is detectable using gas chromatography, mass spectrometry, or a katharometer (thermal conductivity detector).

The purpose of this study is to use alternative passive scalars, namely O, O_2, and He, to generate jet mixture fractions at specific planes in an RQL combustion rig. The mixture fraction data are then used to determine the degree of spatial mixing of chemical species at each of the measurement planes in the combustor. The results are compared to carbon-based f results to demonstrate the viability of a simpler method that requires the analysis of only a single compound to quantify air–fuel mixing.

This study expands on two previous studies by Leong et al.[12,13] In Ref. 12, the setup for reacting tests in an RQL crossflow configuration was described and characterized, and in Ref. 13, the optimal number of jet injection orifices was determined in order to obtain rapid mixing of air jets in a rich crossflow and a uniformly lean, low-temperature mixture at the exit plane of the combustor. Most of the species concentrations required for the carbon- and oxygen-based mass mixture fractions calculations were collected during the second study.[13] In this work, a protocol for the sampling and analysis of the helium tracer gas is established. Tracer gas concentrations are then measured under reacting conditions for a series of RQL modules with a different number of jet orifices. Data are collected at specified planes and spatial coordinates to allow direct comparison with results obtained in Ref. 13.

Experiment

This section describes the experimental setup, the data measurement protocol, and the procedure for calculating carbon-based and tracer gas-based mixture fractions.

Reacting Test Facility

The reacting jet-in-crossflow experimental setup, shown in Fig. 1, has been described in detail in previous papers.[12,13] The upward-fired atmospheric test facility supplies a uniform, fuel-rich composition of gases to the quick-mix section. The quick-mix section
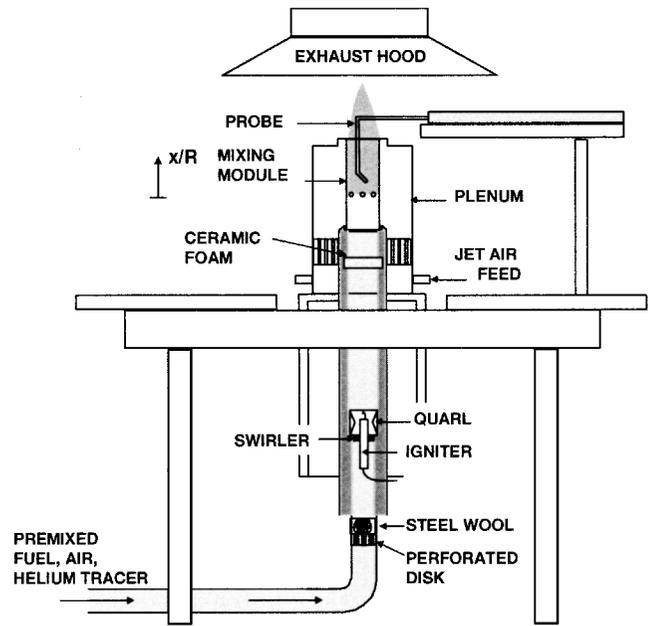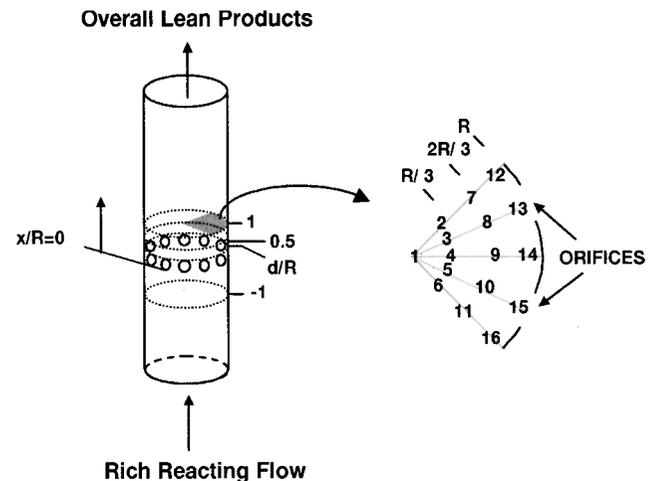

Fig. 1   RQL combustor setup.

Fig. 2   Location of planes and sampling points in RQL combustor module.

utilizes interchangeable quartz tubes containing different jet orifice configurations.

A schematic of the quartz module, shown with the location of the planes of interest, is depicted in Fig. 2. The inner and outer diameters of the tube are, respectively, 80 by 85 mm, and its length is 280 mm. Four different modules were tested, with each one containing a different number of circular orifices (10, 12, 14, or 18) arranged equidistantly around the circumference of the tube. (Note that measurement results for an eight-hole module were reported in Ref. 13, but are not included here because He data were not collected for this module.) The orifice centerlines are located 115 mm from the entrance of the module. The four measurement planes are displaced from the orifice leading edge as follows: one duct radial length upstream ($x/R = -1$), one orifice diameter downstream ($x/R = d/R$), and one-half duct and one duct radial lengths downstream ($x/R = 0.5, 1$). This particular region was chosen because, based on data presented by Leong et al.,[13] this is where the greatest changes in spatial unmixedness occur. For each module tested, point samples were taken from a two-orifice sector at 16 radially equidistant locations (Fig. 2).

Emissions data, required for calculation of carbon- and oxygen-based mixture fractions, were previously presented in Ref. 13 for planes $x/R = -1$, d/R, and 1. Additional emissions samples, using the same setup and procedure as outlined in Refs. 12 and 13, were

collected at $x/R = 0.5$ because intense mixing activity occurs at this plane according to tracer gas data. Emissions were analyzed using the following techniques: CO and CO_2 by non dispersive infrared absorption, O_2 by paramagnetism, and THCs by flame ionization.

The experiment utilizes gaseous propane as the combustion fuel. Propane is first mixed with air to yield a fuel–air equivalence ratio ϕ of 1.67 in the rich combustion section. The rich product generation is described in more detail in Ref. 12. The rich-burning mixture, with average temperatures at the $x/R = -1$ plane of 1500 K, enters the quartz mixing section and undergoes additional reaction with jets of air to result in an overall ϕ of 0.45. The jet air is fed by a plenum that surrounds the rich combustion chamber and the quartz tube. Heat transferred from the combustor to the plenum air heats the jets of air to 480 K before they enter the jet-mixing section.

The rich equivalence ratio is obtained by setting the mass flow rates of propane and crossflow air at 2.96 and 27.5 g/s, respectively. The lean equivalence ratio downstream of the jets requires a total jet mass flow rate of 75.2 g/s. The reference velocity of the total flow is 18 m/s. Based on the temperatures measured in the reacting system, the jet-to-crossflow density ratio is 3.3, and the jet-to-crossflow momentum-flux ratio J is 57. This set of conditions is the same as utilized in previous experiments[12,13] and was selected to fall within the range of gas turbine combustor operating conditions.[4,5,6,23] J is kept constant by keeping the total effective orifice area (903 mm^2) constant for each of the modules tested. This results in different orifice diameters for each orifice number configuration, namely, 12.5, 11.5, 10.6, and 9.4 mm, respectively, for the 10-, 12-, 14-, and 18-hole modules.

Mixture Fraction Determination

The experiment consists of jet airstreams injected into a cylindrically confined crossflow of a fuel-rich mixture of partially reacted propane and air. Based on the method by Jones et al.,[8] the mixture fraction f of the jet fluid is defined as

$$f_i = \frac{Y_i^{\text{crossflow}} - Y_i^{\text{sample}}}{Y_i^{\text{crossflow}} - Y_i^{\text{jet}}} \tag{1}$$

where Y_i represents the mass fractions of a conserved scalar i in the crossflow, jets, and extracted gas sample. The jet mixture fraction tracks the amount of the jet fluid relative to the total mixture at a specific location in the combustor. A gas sample composed entirely of crossflow fluid yields a value of $f = 0$, whereas a sample composed wholly of jet fluid produces a value of $f = 1$.

As shown in Table 1, four different formulations for mass-based jet mixture fraction were examined. In each case, Table 1 lists the measured quantities, the minimum number of unknown variables needed to calculate f, and the assumptions and equations required to solve for these unknowns. The mass-fraction-based calculations using C, O, O_2, and He as the conserved scalars follow the procedure outlined in Ref. 8. Key assumptions in this method are as follows.

1) The combustion gas mixture is composed of major species only, that is, CO, CO_2, O_2, H_2O, N_2, H_2, and THCs, and the respective molar fractions sum to unity.

2) The O_2/N_2 and, thus, O/N ratios are the same in the sample stream as in the combustion air.

3) The sampled C/H molar ratio is the same as in the fuel stream.

Table 1   Formulas and assumptions for calculating jet mixture fraction using different conserved scalars

Conserved scalar	Jet mixture fraction f formula	Known quantities	Unknown quantities	Equations and assumptions
Y_C, Y_O	$f_{Y_C} = 1 - \dfrac{Y_C^{\text{sample}}}{Y_C^{\text{crossflow}}}$ $f_{Y_O} = \dfrac{Y_O^{\text{crossflow}} - Y_O^{\text{sample}}}{Y_O^{\text{crossflow}} - Y_O^{\text{jet}}}$	$X_{\text{CO,dry}}$, $X_{CO_2,\text{dry}}$, $X_{O_2,\text{dry}}$, $X_{\text{THC,dry}}$	$X_{\text{CO,wet}}$, $X_{CO_2,\text{wet}}$, $X_{O_2,\text{wet}}$, $X_{C_3H_8,\text{wet}}$, $X_{C_2H_4,\text{wet}}$, $X_{H_2O,\text{wet}}$, $X_{N_2,\text{wet}}$, $X_{H_2,\text{wet}}$	$X_{i,\text{dry}} = \dfrac{X_{i,\text{wet}}}{1 - X_{H_2O}}$, $i = $ CO, CO_2, O_2, THC C:H = 3:8 O:N = 0.209 : 0.791 $X_{H_2} = 0.65 X_{\text{CO}}$ $\sum_i X_{i,\text{wet}} = 1$ THC = $C_3H_8 + C_2H_4$
Y_{O_2}	$f_{Y_{O_2}} = \dfrac{Y_{O_2}^{\text{sample}}}{Y_{O_2}^{\text{jet}}}$	$X_{\text{CO,dry}}$, $X_{CO_2,\text{dry}}$, $X_{O_2,\text{dry}}$, $X_{\text{THC,dry}}$	$X_{\text{CO,wet}}$, $X_{CO_2,\text{wet}}$, $X_{O_2,\text{wet}}$, $X_{C_3H_8,\text{wet}}$, $X_{C_2H_4,\text{wet}}$, $X_{H_2O,\text{wet}}$, $X_{N_2,\text{wet}}$, $X_{H_2,\text{wet}}$	Same as for Y_C, Y_O $X_{O_2}^{\text{crossflow}} = 0$; $X_{O_2}^{\text{jets}} = 20.9\%$
Y_{He}	$f_{Y_{He}} = 1 - \dfrac{Y_{He}^{\text{sample}}}{Y_{He}^{\text{crossflow}}}$	$X_{\text{CO,dry}}$, $X_{CO_2,\text{dry}}$, $X_{O_2,\text{dry}}$, $X_{\text{THC,dry}}$, $X_{\text{He,dry}}$	$X_{\text{CO,wet}}$, $X_{CO_2,\text{wet}}$, $X_{O_2,\text{wet}}$, $X_{C_3H_8,\text{wet}}$, $X_{C_2H_4,\text{wet}}$, $X_{H_2O,\text{wet}}$, $X_{N_2,\text{wet}}$, $X_{H_2,\text{wet}}$, $X_{\text{He,wet}}$	Same as for Y_C, Y_O $X_{He}^{\text{jets}} = 0$
X_{O_2}	$f_{X_{O_2}} = \dfrac{X_{O_2}^{\text{sample}}}{X_{O_2}^{\text{jet}}} = \dfrac{[O_2]_{\text{sample}}}{20.9\%}$	$X_{O_2,\text{dry}}$	None	$X_{O_2}^{\text{crossflow}} = 0$; $X_{O_2}^{\text{jets}} = 20.9\%$ $M_{\text{sample}} \sim \text{const}$ $X_{O_2,\text{dry}} \propto X_{O_2,\text{wet}}$
X_{He}	$f_{X_{He}} = 1 - \dfrac{X_{He}^{\text{sample}}}{X_{He}^{\text{crossflow}}}$ $= 1 - \dfrac{[He]_{\text{sample}}}{[He]_{\max(x/R=-1)}}$	$X_{\text{He,dry}}$	None	$X_{He}^{\text{jets}} = 0$ Plane $x/R = -1$ is approximately uniform $M_{\text{sample}} \sim \text{const}$ $X_{\text{He,dry}} \propto X_{\text{He,wet}}$

4) To ensure a unique solution to the system of linear equations, that is, equal number of equations and unknowns, two hydrocarbons are included: C_3H_8 as well as C_2H_4, which is a by-product from the pyrolysis of C_3H_8.

5) In the absence of a direct measurement for hydrogen, the H_2 molar fraction is assumed to be proportional to the CO molar fraction.[24,25]

Assumptions 2 and 3 also imply that all major species have equal diffusivities, a reasonable assumption in turbulent flows according to Ref. 11. Assumption 3 is used to infer a molar fraction X for H_2O and, thus, convert the measured dry basis emissions $X_{i,\text{dry}}$ to a wet basis $X_{i,\text{wet}}$ to represent the gases as found in the actual combustion reaction. To perform this basis conversion, Jones et al.[8] uses a matrix formulation of the form

$$AX_{\text{wet}} = X_{\text{dry}} \qquad (2)$$

with a solution given by

$$X_{\text{wet}} = A^{-1}X_{\text{dry}} \qquad (3)$$

where A is an invertible, square matrix, representing the coefficient matrix in the linear system of equations setup using the assumptions listed in Table 1.

The C- and O-based mixture fractions are considered to give the most comprehensive f values because the calculations use all available data and only the five assumptions just listed. In fact, the values for f_{Y_C} and f_{Y_O} will be almost equal given that both fractions are calculated using the same linear equations set under the same assumptions. Thus, all f_{Y_C} results in this study can be considered interchangeable with f_{Y_O}. Note that oxygen atom-based f calculations may be subject to higher percentage uncertainties under certain assumptions due to the subtraction of two nearly equal numbers, that is, in the numerator of the mixture fraction formula.[26]

Using O_2 and He as passive scalars can simplify the determination of f because only data from a single species is needed for the calculation if molar fractions are used. In the case of O_2, under equilibrated lean combustion conditions, the concentration will vary as a direct function of equivalence ratio and, by definition of f, of mixture fraction as well. Any O_2 present in rich regions can be considered as a diluent, which also allows it to serve as quasi-conserved scalar for determining mixture fraction. As shown in Table 1, the ratio of measured to maximum (20.9%) O_2 concentrations can be used to represent $f_{X_{O_2}}$.

In the tracer gas case, the helium was injected into the crossflow air rather than into the jets to maintain a fair comparison between the mixing fields obtained by the earlier carbon atom tracking and the inert tracer method. (In the carbon-based method, the only source of carbon is from the crossflow, not the air jets). Seeding the jet flow, which is 2.5 times the mass flow of the crossflow, would have required helium flow rates that would have quickly depleted available helium supplies during the course of a test. In addition, seeding the crossflow allows for the assessment of its uniformity.

Initially, neon and argon were considered as tracers because their molecular weights and, thus, densities and diffusivities more closely match those of propane and air, as shown in Table 2. Argon, however, has a very high background concentration (9340 ppm) compared to helium (5 ppm) and neon (18 ppm) (Ref. 27) and, thus, was not pursued. Preliminary studies were conducted on the RQL module using the procedure to compare helium and neon as inert tracers. Concentration measurements for both gases injected into the crossflow yielded similar results, suggesting that either could be used as a tracer. Helium has an extensive history as an inert tracer and is much cheaper and more readily available than neon. These practical considerations lead to the choice of helium for use in this experiment.

The injection of the helium tracer into the crossflow, the assumption that the jet airstream contains negligible levels of helium, and the approximation that the helium concentration at the crossflow injection plane is relatively uniform lead to the helium-based jet mixture fraction relationship $f_{X_{He}}$ shown in Table 1. (Variation across the plane was found to be less than 3%.) The value $f_{X_{He}}$ gives the relative change in helium concentration with respect to the maximum

Table 2 Key properties of species used in the determination of jet mixture fraction

Compound	Molar mass M, g/mol	Maximum concentration C, %, dry	Maximum density,[a] g/m^3
Air	28.8	100.0	931.7
CO	12.0	10.0	151.2
CO_2	44.0	13.2	180.0
O_2	32.0	20.9	273.5
C_3H_8	44.1	2.2[b]	38.8
H_2O	34.0	14.8	205.2
He	4.0	0.3	0.5
Ne	20.2	0.2	1.9
Ar	39.9	——	——

[a]Density $\rho = 100(PM/RT)\cdot C$, where $P = 1$ atm, $T = 298$ K, and $R = 8.314$ J/molK.
[b]Measured as total unburned hydrocarbons corrected to propane.

Table 3 Overall constituent mass fractions in zones upstream and downstream of jet mixing section, based on flow rates of fuel, air, and tracer gas

Zone	Helium	Propane	Air
Y_{rich}[a]	4.4×10^{-4}	0.097	0.90
Y_{lean}[b]	1.3×10^{-4}	0.028	0.97

[a]Rich equals helium plus propane plus air.
[b]Lean equals rich plus air jets.

concentration in the plane $x/R = -1$. Ultrapure (99.999% purity) carrier grade helium gas is supplied at a flow rate of 4.5 l/min and injected into the propane stream. This is the minimum flow rate tested under the current operating conditions that produces a distinct signal, which corresponds to a maximum volume concentration of 0.3% of the rich crossflow mixture. The propane–helium mixture is injected into the crossflow air and flows through a 4.3 m mixing length filled with baffles to prepare the gas mixture for combustion. The resulting mass fractions of helium, fuel, and air upstream and downstream of the jet mixing section are noted in Table 3.

First, the mass-fraction-based $f_{Y_{O_2}}$ and $f_{Y_{He}}$ were determined to provide a point of reference to compare to f_{Y_C} and f_{Y_O}. Then, the molar-fraction- (or concentration-)based $f_{X_{O_2}}$ and $f_{X_{He}}$ were calculated. The accuracy of using the molar fraction instead of the mass fraction relies on that most of the sample mass and volume at the measurement planes within the jet injection section are composed of jet air. As a result, one can make the following approximations.

1) The total mass of the sample is constant. (It actually varies by ±4% across the sampling planes.)

2) X_{dry} is linearly proportional to X_{wet}. (The average difference between X_{dry} and X_{wet} is approximately 6% for O_2 and He.)

3) Because of approximations 1 and 2 and given the linear relationship between Y_i and X_i [i.e., $Y_i = (M_i/M_{\text{sample}})X_i$, where M_i is the molar mass of species i and M_{sample} is the molar mass of the sample], $f_{Yi,\text{wet}} \cong f_{Xi,\text{dry}}$. The maximum deviation of f_X with respect to f_Y was calculated to be ±0.08 for f_{X_C}, ±0.03 for $f_{X_{O_2}}$, and ±0.05 for $f_{X_{He}}$.

The procedure for collecting the CO, CO_2, O_2, and THC emissions used to determine f_{Y_C}, f_{Y_O}, $f_{Y_{O_2}}$, and $f_{X_{O_2}}$ was outlined in Refs. 12 and 13. The experimental component in this paper involves the measurement of the helium tracer gas used for calculating $f_{Y_{He}}$ and $f_{X_{He}}$.

Inert Gas Tracer Sampling Protocol

The injection and sampling train of the helium tracer system is shown in Fig. 3. Gas samples are extracted from the flowfield and drawn through a water-cooled probe with a pump. After condensing water from the sample through an impinger submersed in an ice bath, the gas is sent to a gas chromatograph [Hewlett–Packard (HP) 5890 Series II] to measure the helium concentration. When a sample analysis is initiated, the volume of gas contained in the 250-μl sample loop of the gas chromatograph is injected into the
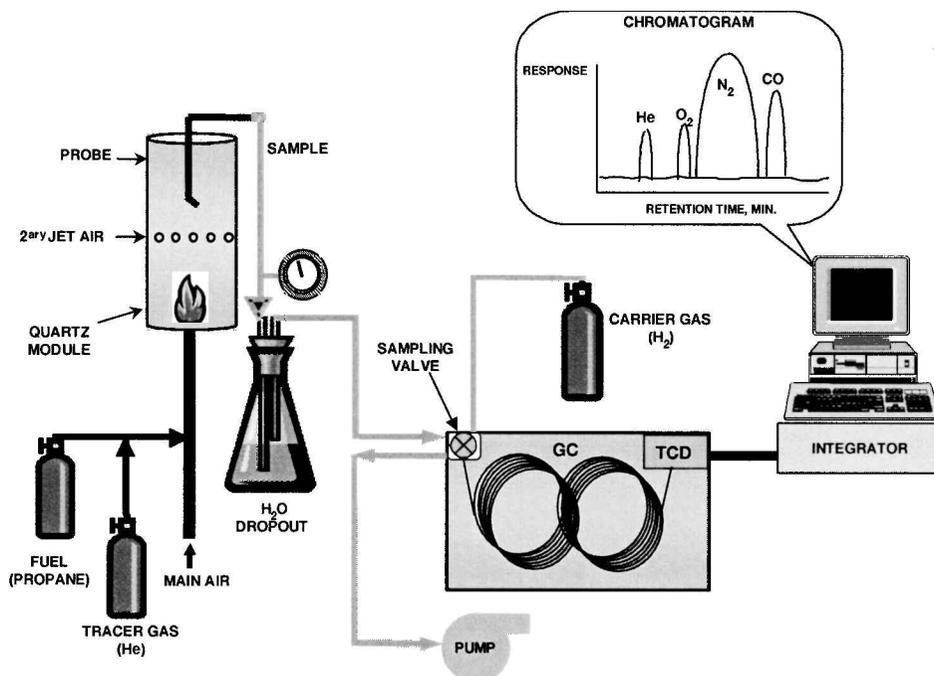
Fig. 3   Setup of helium injection system, sampling train, and analysis system.

column, while the balance of the extracted gas is diverted through a flow bypass.

The gas chromatograph setup is optimized to obtain the fastest elution time of the helium tracer gas with acceptable chromatographic separation. To separate the helium atoms from the heavier molecules of fuel, air, and combustion products, the sample flows through two columns, connected in series. Both columns, manufactured by J&W Scientific Inc., are megabore, capillary, gas solid (GS) phase columns, with an inner diameter of 0.54 mm and a length of 30 m. Ultrapure grade hydrogen (99.999% H_2 concentration) is used as the carrier gas to minimize the sample elution time, as well as prevent chromatographic interference from H_2 generated from the combustion of fuel-rich mixtures.

Chromatographic separation takes place in two stages. The gas sample is injected into a GS-Q® column before flowing through a GS-MolSieve® column. The GS-Q column separates hydrocarbon molecules such as methane, ethane, and propane, whereas the GS-MolSieve column separates compounds of low molecular weight, including helium, neon, oxygen, nitrogen, and carbon monoxide. The effects of the hydrocarbon molecules on the sensitivity of the GS-MolSieve column necessitated the use of timed valve switching. The valve controlling the flow circuitry is switched 30 s after the helium enters the GS-MolSieve column and interrupts the flow between the GS-Q and GS-MolSieve columns. The carrier gas flow through the GS-Q column is reversed (backflushed) to flush the sample containing the hydrocarbon molecules out of the system, while the helium continues to separate from the remainder of the sample in the GS-MolSieve column as it moves toward the detector.

To detect helium, the gas chromatograph uses a thermal conductivity detector (TCD). The TCD detects the difference in the thermal conductivities of the eluted sample and the carrier gas, generating a differential voltage signal. The output from the TCD is connected to an integrator (Spectra Physics DataJet), which in turn is connected to a computer. The WINner on Windows software package by Thermo Separation Products was used to integrate the resulting chromatograms. From helium calibration runs performed before and after each test, a constant of proportionality is obtained to quantify the integrated areas under the peaks in terms of volumetric concentration.

Completion of the analysis requires approximately 1.5 min, followed by 30 s to flush out the columns to prepare them for the next sample. The gases elute in the following order: helium at 0.59 min, air at 0.66 min, and CO at 0.74 min.
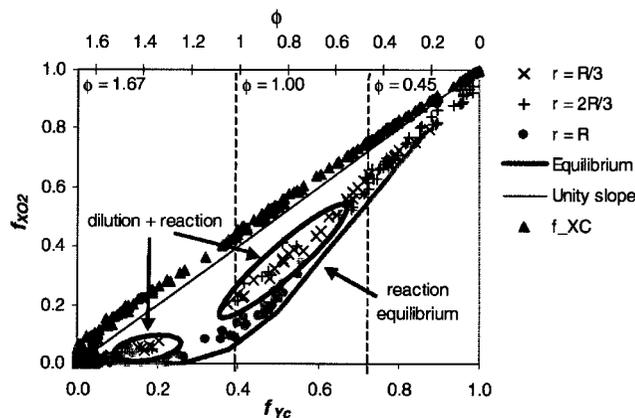

Fig. 4   Comparison between carbon mass fraction-based f_{Y_C} and oxygen concentration-based $f_{X_{O_2}}$ jet mixture fractions: $\times$, $r = R/3$; $+$, $r = 2R/3$; $\bullet$, $r = R$; ——, equilibrium; ——, unity slope; and $\blacktriangle$, f_{X_C}.

Results and Discussion

Mixture Fraction

The simplified molar mixture fraction formulations proposed in this paper, namely, $f_{X_{O_2}}$ and $f_{X_{He}}$, are plotted in Figs. 4 and 5 vs f_{Y_C} and equivalence ratio ϕ. Figure 4 also graphs f_{X_C} vs f_{Y_C}, showing that the molar-fraction-based mixture fraction slightly overpredicts f_{Y_C} by approximately 5%. The equivalence ratio was calculated from f_{Y_C} according to Jones et al.[11] using the following formula:

$$\phi = [\xi/(1 - \xi)]\left(1 + Y_{N_2}\big/Y_{O_2}\right)\left(5 M_{O_2}\big/M_{C_3H_8}\right) \qquad (4)$$

where

$$\xi = Y_C^{\text{sample}}\big/Y_C^{\text{fuel}} = (1 - f)\left(M_{C_3H_8}\big/M_{\text{crossflow}}\right) \qquad (5)$$

Figures 4 and 5 include data collected at all of the measurement planes for the four test modules. The data are grouped in terms of sampling radius to better explain certain results. Grouping by module type or sampling plane did not yield any identifiable trends. Figures 4 and 5 show that $f_{X_{O_2}}$ and $f_{X_{He}}$ correlate positively with f_{Y_C}, but they exhibit significant deviations from the carbon-based
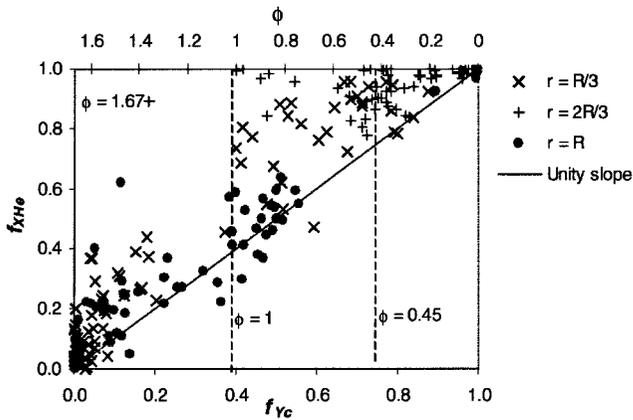
Fig. 5 Comparison between carbon mass fraction-based f_{Y_C} and helium concentration-based $f_{X_{He}}$ jet mixture fractions: $\times$, $r = R/3$; $+$, $r = 2R/3$; $\bullet$, $r = R$; and ——, unity slope.

Table 4 Standard error σ and coefficients of determination R^2 for O_2- and He-based mixture fractions f_X and spatial unmixedness U_S with respect to f_{Y_C} and U_{S,Y_C}

Parameter	$f_{X_{O_2}}$ [a]	$f_{X_{He}}$ [a]	$U_{S,X_{O_2}}$	$U_{S,X_{He}}$
σ	0.09	0.12	0.06	0.08
R^2	0.94	0.90	0.96	0.93

[a]Except for points at the upstream plane $x/R = -1$ where f is uniform and approximately zero, σ and R^2 values for jet mixture fraction f were calculated using all of the data obtained for each module.

mixture fraction. Experimental uncertainties for $f_{X_{He}}$, $f_{X_{O_2}}$, and f_{Y_C} are, respectively, ± 0.08, ± 0.01, and ± 0.02. The apparent gap in data points in the region of $0.2 < f < 0.4$, which corresponds to near-stoichiometric combustion, illustrates the staging in RQL combustion that causes the reaction to shift from $\phi = 1.67$ to $\phi = 0.45$ by quick mixing to avoid hot stoichiometric pockets.

In the case of $f_{X_{O_2}}$, the values underpredict f_{Y_C}. Two trends are evident in Fig. 4, one corresponding to combustion equilibrium (predicted by the NASA equilibrium code) and the other to jet dilution and quenching of the reaction. The dilution effect is linear in both the slightly rich and slightly lean regimes. Extra scatter in the data around the knee at near-stoichiometric conditions, that is, for $0.3 < f < 0.5$, indicates nonequilibrium conditions, resulting in higher than equilibrium O_2 and CO values. Figure 4 suggests that the deviation occurs away from the walls, that is, $r = R/3, 2R/3$, from which one can surmise that the nonequilibrium conditions are probably due to the intense, turbulent, quick-mix transition from rich to lean conditions following jet injection. Near the edges of the combustor, that is, $r = R$, where jet interaction is less, equilibrium conditions prevail. Thus, in addition to the usefulness of O_2 concentration profiles to track jet trajectories and determine the general zones where reacting and mixing processes are occurring (as shown in Ref. 12), one can use O_2 to distinguish between the two processes.

As seen in Fig. 5, the $f_{X_{He}}$ data overpredict and show considerable scatter with respect to f_{Y_C}. The overprediction may be attributed to 1) the higher molecular and turbulent diffusivity of He with respect to the other major products of combustion and 2) the use of the molar fraction rather than the mass fraction, which can introduce a positive bias of up to 0.05 for high mixture fraction values. The data collected at $r = R$, where, as noted earlier, equilibrium conditions hold, appear to correlate well with f_{Y_C}. However, once the jet interaction is thrust into the picture, the tracer may be unable to follow the high-momentum jet trajectories. In Ref. 12, it was shown that overpenetrating jets displace the rich reacting fluid toward the walls, while the jet mass migrates and accumulates in the central core of the combustor. This is corroborated by that the flows at $r = 2R/3$ and $R/3$ seem either to trap completely ($f = 0$) or to exclude totally ($f = 1$) the He tracer molecules.

The scatter, on the other hand, may be attributed to a variety of factors, in addition to experimental uncertainty. The high turbulence at the jet–crossflow interface due to reacting and mixing processes can cause large spatial–temporal fluctuations and asymmetries in the mixture fraction. Density differences between He and the other major combustion products can result in large differences in momentum flows and kinematic eddy viscosities (turbulent momentum diffusivities), which in turn affects the He transport in the turbulent eddies in the mixing regions. Previous isothermal experiments used He concentrations of at least 1%, whereas, in this study, the concentrations were less than 0.3%. Although these values were chosen to minimize a potential diluent effect, perhaps, in hindsight, the concentration levels were too low for use in reacting conditions. Finally,

there is the possibility of small offsets in the relative position of the sampling probe between runs. As a result of the extreme scattering in the He data, this technique would need further refinement before it would be seen as amenable for reliably determining mixture fraction.

To better quantify linear correlations between the mixture fraction data, two parameters were selected: 1) standard errors σ, which give the magnitude of typical deviation from the estimated linear regression line, and 2) coefficients of determination R^2, which represent the proportion of a data set that can be explained by the linear regression model. These values are presented in Table 4. Thus, σ and R^2 quantify the data scatter, whereas the regression curve fit would quantify the actual agreement between the various mixture fraction formulations. The statistical analysis confirms the better fit for the O_2 data, whose σ is on the order of half of that of the He data. The analysis also shows the He data to be consistently overpredicting f_{Y_C} by $\sim 10\%$ and O_2 underpredicting f_{Y_C} also by $\sim 10\%$.

To better visualize and compare the various scalars, stacked sector plots, presented in Figs. 6–8 were generated to show the evolution of the scalar flowfield through the modules in terms of f_{Y_C} (reproduced from Ref. 13), $f_{X_{O_2}}$, and $f_{X_{He}}$. Note that the flow is upward such that the farthest upstream plane is at the bottom, and the farthest downstream plane is at the top. The $f_{X_{O_2}}$ and $f_{X_{He}}$ results suggest a qualitative match with the f_{Y_C} data. All plots show uniformity at $x/R = -1$ and similar trends in jet penetration at $x/R = d/R$.

The ideal, fully mixed case occurs when the jets mix uniformly with the crossflow. One can calculate the ideal jet mixture fraction by substituting the jet and crossflow mass fractions, based on input mass flow rates, into Eq. (1) to yield an f of 0.714. The f_{Y_C} stack plots in Fig. 6 indicate that such a region occurs at the plane $x/R = 1$. The $f_{X_{He}}$ data shown in Fig. 8 indicate poorer mixing with most of the downstream flow composed of jet fluid. The $f_{X_{O_2}}$ data plotted in Fig. 7, on the other hand, suggest only a narrow band of good mixing, but with crossflow fluid still present in the central and outer rings of the combustor. Both helium- and oxygen-based f data show steeper gradients than their equivalent carbon-based values.

Spatial Unmixedness

To determine the effectiveness of the tracer gas method in assessing overall mixing, one can calculate spatial unmixedness U_S based on f. U_S is the normalized variance quantifying planar mixing and is defined by

$$U_S = f_{\text{var}}/f_{\text{av}}(1 - f_{\text{av}}) \qquad (6)$$

where f_{var} refers to the variance of all f in a plane that deviate from f_{av}, the area-weighted average jet mixture fraction specific to each plane.[28] U_S values lie between 0 (perfect fuel–air mixing) and 1 (totally unmixed system). Figure 9 reveals that $U_{S,X_{O_2}}$ and $U_{S,X_{He}}$ correlate reasonably well with each other and with U_{S,Y_C}. The same data are plotted vs axial distance x/R in Fig. 10. At the orifice trailing edge, that is, where $x/R = d/R$, where all of the jet mass is injected, U_S reaches a peak and then decreases downstream as the jets mix with the crossflow. It appears that the procedure of calculating a planar variance and then normalizing the result eliminates some of the scatter and discrepancies seen in the point measurement mixture fraction data. (See Table 4 for the corresponding σ and R^2 regression values.)
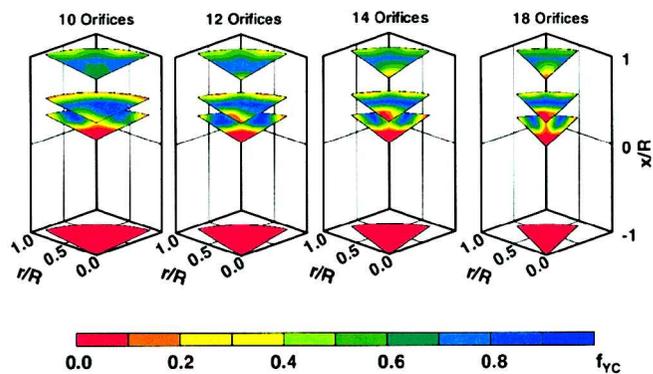
Fig. 6 Carbon mass fraction-based f_{Y_C} mixture fraction fields.
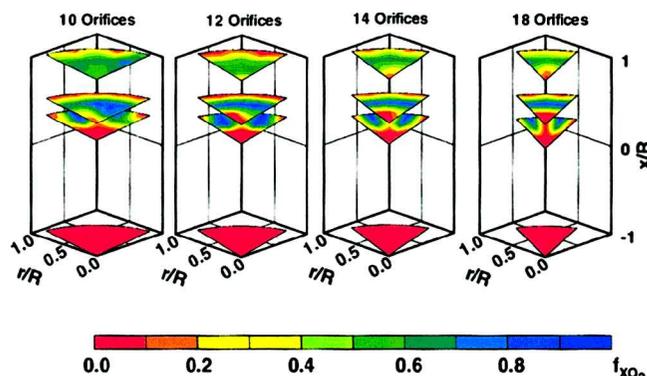

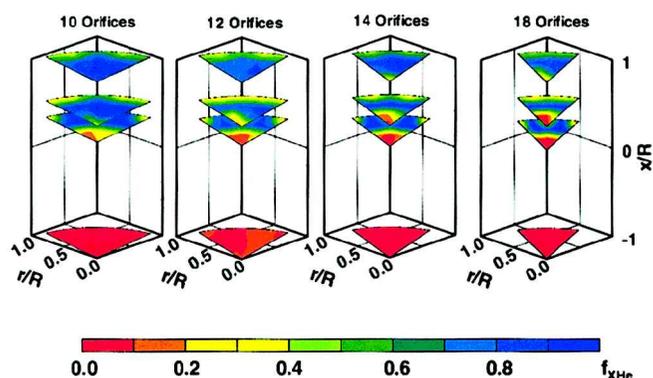Fig. 7 Oxygen concentration-based $f_{X_{O_2}}$ mixture fraction fields.

Fig. 8 Helium concentration-based $f_{X_{He}}$ mixture fraction fields.

Comparison of Conserved Scalar Measurement Methodologies

The quantitative results discussed warrant a brief discussion of the relative advantages and disadvantages of each technique. The carbon-based method requires several emissions analyzers for simultaneous species measurement, but also permits localized characterization of pollutant emissions, which can then be evaluated with respect to local mixing efficiency. This method is also the most comprehensive technique because all major species are included in the mixture fraction calculation.

The oxygen-based method only uses a single O_2 analyzer, but would require a backcalculation to correct for dilution or lean combustion to extract the actual local mixture fraction. However, this method appears to be the simplest technique for the rapid characterization of local jet mixture fraction and spatial unmixedness, despite that the effective use of O_2 as a passive scalar is predicated on the assumption that O_2 is present in only one of the two flows. Both the C-based and O_2-based methods allow one to assess the degree of reaction vs mixing occurring between the two streams.

The helium-based method, on the other hand, only provides mixing information and requires the added complication of metering
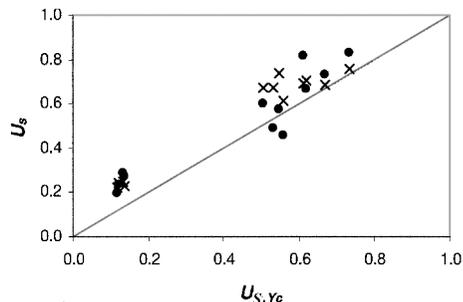

Fig. 9 Comparison between carbon mass fraction-based U_{S,Y_C}, oxygen concentration-based $U_{S,X_{O_2}}$, and helium-concentration based $U_{S,X_{He}}$ spatial unmixedness for all modules: ●, $U_{S,X_{He}}$, and ×, $U_{S,X_{O_2}}$.

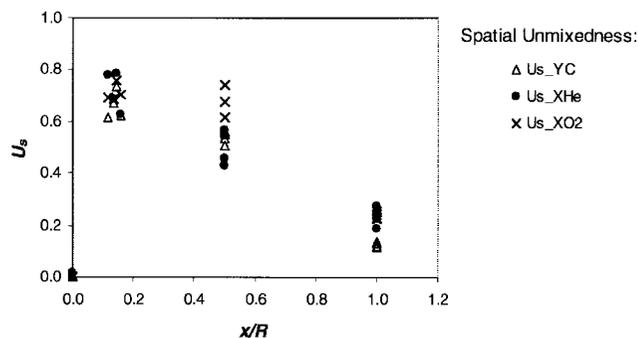Fig. 10 Spatial unmixedness values at each measurement plane: △, U_{S,Y_C}; ●, $U_{S,X_{He}}$; and ×, $U_{S,X_{O_2}}$.

and injecting a tracer gas. However, He-based measurements could serve as simpler diagnostic substitute to quantify mixing in the absence of a full emissions measurement console. Furthermore, this method could be used to verify independently the carbon-based mixture fraction calculations. The gas chromatographic analysis used for He detection could also be configured to measure emissions and helium simultaneously. Hence, using a single sampling system, one could then apply any of the described methods to characterize the mixing field.

If helium or other inert tracer gases are to be used in future experiments to determine mixture fractions, the effect of tracer gas density and diffusivity on its dispersion in the mixing field needs to be investigated. It would be useful to determine the linearity of the tracer injection method because a normalized response curve should be independent of quantity of tracer injected.[16] In addition, the sensitivity and repeatability of the tracer gas analysis system should be improved, for example, by ensuring a constant pressure sample injection and using multipoint calibration for the gas chromatographic analysis. Use of a commercial helium detector, instead of gas chromatography, would also help to overcome sensitivity issues, as well as speed up the gas analysis.

Conclusions

This study investigated the use of passive scalars, namely, the carbon atom, the oxygen molecule, and helium (as an inert tracer gas) to quantify jet mixing in a reacting crossflow. The results show that mole fraction O_2- and He-based jet mixture fractions correlate positively but exhibit significant deviations from the mass fraction C-based localized jet mixture fraction. In general, the O_2-based mixture fraction underpredicts the C-based mixture fraction due to jet dilution and combustion, with additional discrepancies near $\phi = 1$ due to nonequilibrium conditions in the RQL quick-mixing zone. The He tracer, on the other hand, overpredicts the C-based mixture fraction, possibly due to differences in density and diffusivity, and exhibits significant scatter most likely attributable to differences in gas density and turbulent diffusivity. However, the data show a much better quantitative agreement between the O_2-, He-, and

C-based methods when assessing planar mixing fields in terms of spatial unmixedness. Although the combustor rig was designed to test RQL combustion, the results of this experiment can potentially be applied more generally as a diagnostic to assess air–fuel mixing in other types of reacting systems.

Acknowledgment

References

[1] Appleton, J. P., and Heywood, J. B., "The Effects of Imperfect Fuel-Air Mixing in a Burner on NO Formation from Nitrogen in the Air and the Fuel," *Fourteenth International Symposium on Combustion*, The Combustion Inst., 1972, pp. 777–786.

[2] Fric, T. F., "Effects of Fuel–Air Unmixedness on NO_x Emissions," *Journal of Propulsion and Power*, Vol. 9, No. 5, 1993, pp. 708–713.

[3] Lyons, V. J., "Fuel/Air Nonuniformity-Effect on Nitric Oxide Emissions," *AIAA Journal*, Vol. 20, No. 5, 1982, pp. 660–665; also NASA TP 1798, Nov. 1981.

[4] Holdeman, J. D., "Mixing of Multiple Jets with a Confined Subsonic Crossflow," *Progress in Energy and Combustion Science*, Vol. 19, No. 1, 1993, pp. 31–70; also NASA TM 104412, June 1991.

[5] Holdeman, J. D., Liscinsky, D. S., Oechsle, V. L., Samuelsen, G. S., and Smith, C. E., "Mixing of Multiple Jets With a Confined Subsonic Crossflow: Part I—Cylindrical Duct," *Journal of Engineering for Gas Turbines and Power*, Vol. 119, No. 4, 1997, pp. 852–862; also NASA TM 107185, June 1996.

[6] Holdeman, J. D., Liscinsky, D. S., and Bain, D. B., "Mixing of Multiple Jets With a Confined Subsonic Crossflow: Part II—Opposed Rows of Orifices in a Rectangular Duct," *Journal of Engineering for Gas Turbines and Power*, Vol. 121, No. 3, 1999, pp. 551–562; also NASA TM 107461, June 1997.

[7] Margason, R. J., "Fifty Years of Jet in Cross Flow Research, Computational and Experimental Assessment of Jets in Cross Flow," *Proceedings of the NATO AGARD Conference*, CP-534, April 1993, pp. 1.1–1.40.

[8] Jones, W. P., McDonell, V., McGuirk, J. J., Milosavljevic, V. D., Taylor, A. M. K. P., and Whitelaw, J. H., "The Calculation of Mean Mixture Fractions in Turbulent Non-Premixed Methane Flames from Aspiration-Probe Measurements," Dept. of Mechanical Engineering, Rept. TF/93/13, Imperial College of Science, Technology and Medicine, U.K., March 1993.

[9] Stårner, S. H., Kelman, J. B., Masri, A. R., and Bilger, R. W., "Multispecies Measurements and Mixture Fraction Imaging in Turbulent Diffusion Flames," *Experimental Fluid and Thermal Science*, Vol. 9, No. 2, 1994, pp. 119–124.

[10] Goix, P. J., Leonard, K. R., Talbot, L., and Chen, J. Y., "Direct Measurement of Mixture Fraction in Reacting Flow Using Rayleigh Scattering," *Experiments in Fluids*, Vol. 15, No. 4–5, 1993, pp. 247–254.

[11] Jones, W. P., and Toral, H., "Temperature and Composition Measurements in a Research Gas Turbine Combustion Chamber," *Combustion Science and Technology*, Vol. 3, No. 5–6, 1983, pp. 249–275.

[12] Leong, M. Y., Samuelsen, G. S., and Holdeman, J. D., "Mixing of Air Jets with a Fuel-Rich, Reacting Crossflow," *Journal of Propulsion and Power*, Vol. 15, No. 5, 1999, pp. 617–622; also NASA TM 107430, April 1997.

[13] Leong, M. Y., Samuelsen, G. S., and Holdeman, J. D., "Optimization of Jet Mixing into a Rich, Reacting Crossflow," *Journal of Propulsion and Power*, Vol. 16, No. 5, 2000, pp. 729–735; also NASA TM-97-206294, Dec. 1997.

[14] Gupta, S. K., Moravcik, P. S., and Lau, L. S., "Use of Injected Helium as a Hydrological Tracer," *Hydrological Sciences Journal*, Vol. 39, No. 2, 1994, pp. 109–119.

[15] Rasmussen, T. C., "Laboratory Characterization of Fluid Flow Parameters in a Porous Rock Containing a Discrete Fracture," *Geophysical Research Letters*, Vol. 22, No. 11, 1995, pp. 1401–1404.

[16] Paris, J. R., Ross, P. N., Dastur, S. P., and Morris, R. L., "Modeling of the Air Flow Pattern in a Countercurrent Spray-Drying Tower," *Industrial and Engineering Chemistry, Process Design and Development*, Vol. 10, No. 2, 1971, pp. 157–164.

[17] Adachi, M., Hirano, T., and Ishida, K., "Measurement of Exhaust Flow Rate: Helium Trace Method with a Mass Spectrometer," Society of Automotive Engineers, SAE Paper 971020, Feb. 1997.

[18] Rastogi, A. K., and Whitelaw, J. H., "The Effectiveness of Three-Dimensional Film-Cooling Slots—I. Measurements," *International Journal of Heat and Mass Transfer*, Vol. 16, No. 9, 1973, pp. 1665–1681.

[19] Heitor, M. V., and Whitelaw, J. H., "Velocity, Temperature, and Species Characteristics of the Flow in a Gas-Turbine Combustor," *Combustion and Flame*, Vol. 64, No. 1, 1986, pp. 1–32.

[20] Toral, H., and Whitelaw, J. H., "Velocity and Scalar Characteristics of the Isothermal and Combusting Flows in a Combustor Sector Rig," *Combustion and Flame*, Vol. 45, No. 3, 1982, pp. 251–272.

[21] Khan, Z. A., and Whitelaw, J. H., "Vector and Scalar Characteristics of Opposing Jets Discharging Normally Into a Cross-Stream," *International Journal of Heat and Mass Transfer*, Vol. 23, No. 12, 1980, pp. 1673–1680.

[22] Thayer, W. J., III, and Corlett, R. C., "Gas Dynamic and Transport Phenomena in the Two-Dimensional Jet Interaction Flowfield," *AIAA Journal*, Vol. 10, No. 4, 1972, pp. 488–493.

[23] Lefebvre, A. H., *Gas Turbine Combustion*, 2nd ed., Taylor and Francis, Philadelphia, 1999, pp. 111–119.

[24] Dibble, R. W., Masri, A. R., and Bilger, R. W., "The Spontaneous Scattering Technique Applied to Nonpremixed Flames of Methane," *Combustion and Flame*, Vol. 67, No. 3, 1987, pp. 189–206.

[25] Masri, A. R., Bilger, R. W., and Dibble, R. W., "Turbulent Non-Premixed Flames of Methane Near Extinction: Mean Structure from Raman Measurements," *Combustion and Flame*, Vol. 71, No. 3, 1988, pp. 245–266.

[26] Saito, K., Williams, F. A., and Gordon, A. S., "Structure of Laminar Coflow Methane–Air Diffusion Flames," *Journal of Heat Transfer*, Vol. 108, No. 3, 1986, pp. 640–648.

[27] Seinfeld, J. H., and Pandis, S. N., *Atmospheric Chemistry and Physics*, Wiley, New York, 1998, p. 22.

[28] Liscinsky, D. S., True, B., and Holdeman, J. D., "Experimental Investigation of Crossflow Jet Mixing in a Rectangular Duct," AIAA Paper 93-2037, July 1993; also NASA TM 106152, 1993.